Automatic Positioning of Features in Low-Contrast Fluoroscopic Images

Mélissa Jourdain *
Université de Montréal and Université de la Méditerranée

Jean Sequeira †
Université de la Méditerranée, Image et Modèle

Jean Meunier‡
Université de Montréal

Jean-Claude Tardif §
Montreal Heart Institute

Jean-Marc Boï ¶
Université de la Méditerranée, Image et Modèle

Abstract

During an Intravascular Ultrasound (IVUS) intervention, a catheter with an ultrasound transducer is introduced in the body through a blood vessel and then pulled back to image a sequence of vessel cross-sections. To position the IVUS images in space, some researchers have proposed to add a single view fluoroscopy image sequence to recover the 3D positions of the IVUS transducer during its pullback. We present here a method that enables the tracking of the IVUS transducer and its guidewire in the artery in the fluoroscopic images. The technique uses both a feature tracking method based on structure tensor for some marker points along the guidewire, and a constrained snake approach for the whole catheter. Our approach copes with the low contrast and noise intensity in the fluoroscopic image sequences

Keywords: feature points detection, snake algorithm, fluoroscopic images, intravascular ultrasound system (IVUS)

1 Introduction

Among all pathologies affecting the modern world, cardiovascular diseases are in the forefront. One of the most common cardiovascular problems is coronary atherosclerosis, the build up of plaque (a combination of cholesterol, cellular waste and other materials) on artery walls. The investigation of the severity of coronary atherosclerosis is therefore very important for the diagnosis and therapeutic strategy that will be undertaken.

Intravascular ultrasound (IVUS) produces unique echographic images showing the cross-section of coronary arteries. These images reveal clearly the lumen, walls and plaque and offer a powerful tool for diagnostic purposes. During an Intravascular Ultrasound (IVUS) intervention, a catheter with an ultrasound transducer is introduced in the body through a blood vessel and then pulled back to image a sequence of vessel cross-sections. Those images are hard to analyze since they do not provide information about the 3D geometry of the vessels which is crucial for diagnosis. To get these measurements, one has to first retrieve the 3D trajectory of the IVUS transducer in the vessel to finally align the IVUS cross-section frames of the arteries along the trajectory.

Several techniques investigate this last problem. Conventional 3D IVUS assumes a straight vessel, neglecting curvature and torsion of coronary arteries [J.Roelandt et al. 1994]. Others combine IVUS to angiography. This last modality is a radiography of blood vessels after the injection of a radio-opaque substance. In [Laban et al. 1995],[Slager et al. 2000] and [Wahle et al. 1999], the authors calibrate a biplane angiography system to retrieve the 3D trajectory of the IVUS transducer in the vessel. This kind of methods are complicated to operate and are not always available in clinical center.

Recently, methods based on a single-plane fluoroscopy have been investigated. This modality provides a smaller amount of X-ray on the patient to the detriment of the image quality and does not involve injection of radio-opaque substance in the patient. In the figure 1, we present an image example of fluoroscopy image. To eliminate the amibiguity induced in 3D reconstruction when only one projection is available, they use *a priori* information such as the transducer length and its 2D projection [Sherknie et al. 2005] or its constant pullback speed [Jourdain et al. 2004]. In these cases, we have to retrieve the 3D position of the transducer in each frame of the fluoroscopy sequence. This kind of approach is not easy to apply in clinical cases since the movement of the transducer is not only influenced by the motorized pullback but also by the breathing and cardiac cycle or other arbitrary movements of the patient during the examination. In order to obtain reliable results in 3D reconstruction for single-plane approaches, one has to first perform registration over the images of the sequences. At the end, the only remaining movement should be the motorized pullback of the transducer.

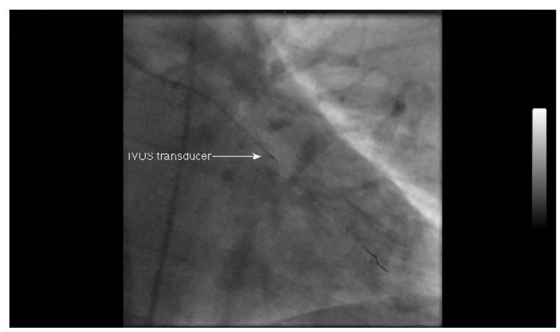

Figure 1: *An image example of fluoroscopy.*

In [Sherknie et al. 2005], they manually tracked the important components in the fluoroscopic images which is a long and non accurate process. In [Jourdain et al. 2004], they track the features by using an algorithm based on temporal intensity difference, which can lead to bad results in case the global intensity changes over time or too much noise is present in the images. In both cases, they had to apply a post-filtering process of the obtained tracked coordinates. In this paper, we present a new method that performs semi-automatic detection of the whole transducer guide in fluoroscopic sequences of images, the first step to elaborate a registration method.

It retrieves the position of the guide even with the poor constrast encounter in fluoroscopic images without needing any post-filtering of the obtained points positions along the guide, opposite to [Jourdain et al. 2004] and [Sherknie et al. 2005]. Our method consists in using a modified snake algorithm based on a local coherence measure found in the image, opposite to standard snake methods based on intensity gradient. It requires approximate positions of different feature points along the guide for the first frame of the sequence in order to position the whole guide. For all the other frames in

*e-mail: jourdaim@iro.umontreal.ca
†e-mail:Jean.Sequeira@univmed.fr
‡e-mail:meunier@iro.umontreal.ca
§e-mail:jean-claude.tardif@icm-mhi.org
¶e-mail:Jean-Marc.Boi@esil.univ-mrs.fr

the sequence, the guide is positionned automatically. Our method manages to find the transducer guide even though some part of it sometimes disappear in the background of the images due to the low contrast.

We first present a tracking method for different feature points along the guide, that is used to restrain the position of the tracked transducer guidewire. We then present a modified snake algorithm constrained by several anchor points corresponding to feature points along the catheter. We also describe a technique that provides an automatic adjustment of the parameters involved in snake-based methods.

2 Tracking algorithm for Feature Points of the IVUS Transducer Guidewire

We first developed a tracking algorithm for the different characteristic points identified in the figure 2. In this section we present the structure tensor that is involved in the positioning of the feature points along the transducer guide. We then describe the tracking method used.

2.1 Structure Tensor

The structure tensor as presented in [Weickert 1998] measures the behavior of the gradient orientation in a neighborhood of each pixel in a given image. It provides a reliable method to distinguish feature areas, such as corners or edges, from constant areas. It also yields direction and magnitude of the highest and smallest intensity fluctuations for a given pixel.

To do so, we used the matrix J_0 defined as follow:

$$J_0(\nabla u_{x,y}) = \nabla u_{x,y} \otimes \nabla u_{x,y} = \nabla u_{x,y} \nabla u^t_{x,y} \tag{1}$$

where:

1. $\nabla u_{x,y} = (I_x, I_y)$ corresponds to the intensity gradient for the pixel (x, y) of the image I.
2. I_x is the gradient in the x-direction.
3. I_y is the gradient in the y-direction.

The matrix J_0 has an orthonormal basis formed by its eigenvectors v_1 and v_2 such as

1. $v_1 \parallel \nabla u_{x,y}$ gives the direction with the most important intensity fluctuations in the image
2. $v_2 \perp \nabla u_{x,y}$ gives the coherence direction along which we find the most constant intensity.

The eigenvalues μ_1 and μ_2 of the matrix J_0 give the image contrast in the direction of their corresponding eigenvectors (v_1 and v_2). A high eigenvalue corresponds to high grey level fluctuations in the image along the direction of its associated eigenvector ([Weickert 1998].

In order to establish a measure of the coherence in the image for the pixel (x, y), we compute the difference between the eigenvalues μ_1 and μ_2 of the matrix $J_0(\nabla u_{x,y})$. This provides an easy way to determine if the area that contains a pixel (x, y) is constant or not. For example, we can have these configurations:

1. $\mu_1 = \mu_2 = 0$: the area is constant since there is no gray level fluctuations in both directions v_1 and v_2.
2. $\mu_1 \gg \mu_2 = 0$: the pixel (x, y) is part of a straight edge since there is intensity variations only along the gradient direction v_1 (figure 3 **(a)**) .
3. $\mu_1 \geq \mu_2 \gg 0$: the pixel (x, y) is on a corner since there is gray level fluctuations in all directions (figure 3 **(b)**).

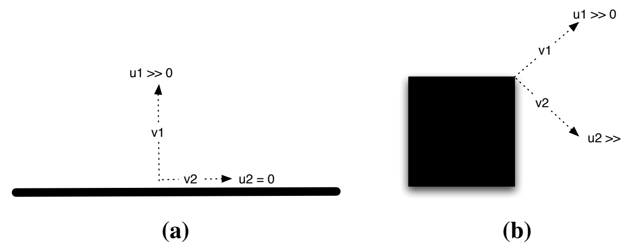

Figure 3: *In* **(a)** *and* **(b)** *respectively, an image composed of one black straight edge and a black square on a white background. The eigenvalues and eigenvectors of the matrix J_0 are presented for a feature point in both image.*

The coherence C that determines whether a pixel is part of a constant area or not, is defined as follow:

$$C = (\mu_1 - \mu_2)^2 \tag{2}$$

We can classify the pixels of the highest coherence to be feature points.

In the figure 4**(a)** and **(b)**, a small window showing a marker on the IVUS transducer guidewire is presented with its associated coherence surface. The measured coherence is significantly higher on the contour of the marker.

2.2 Processing of Positions of Feature Points Using Structure Tensor

We have elaborated a method that tracks the feature points of the figure 2 throughout a fluoroscopic image sequence. The algorithm only needs, as input, the approximate positions of the tracked sructures. For each image, the centroid of each of the feature structures is tracked. The coherence surface $(x, y, C(x, y))$ for the window that corresponds to a certain neighborhood of the approximate position for each of the feature points is calculated. (x, y) representing a pixel and $C(x, y)$, the coherence measured in the neighborhood of this pixel.

From this coherence surface, one can determine a set of points with a high probability on the contour of a structure in an image. A point (x, y) is considered as a feature point if the value of its coherence C responds to the following criterion:

$$C \geq \overline{C} + n * C_\sigma \tag{3}$$

where $\overline{C}$ and C_σ are respectively the mean and standard deviation of the coherence surface computed for a window in an image. We fixed $n = 3$ to detect points with significantly high coherence. This last value was set to make sure that only pixels with high enough coherence would be considered in the process of the feature points

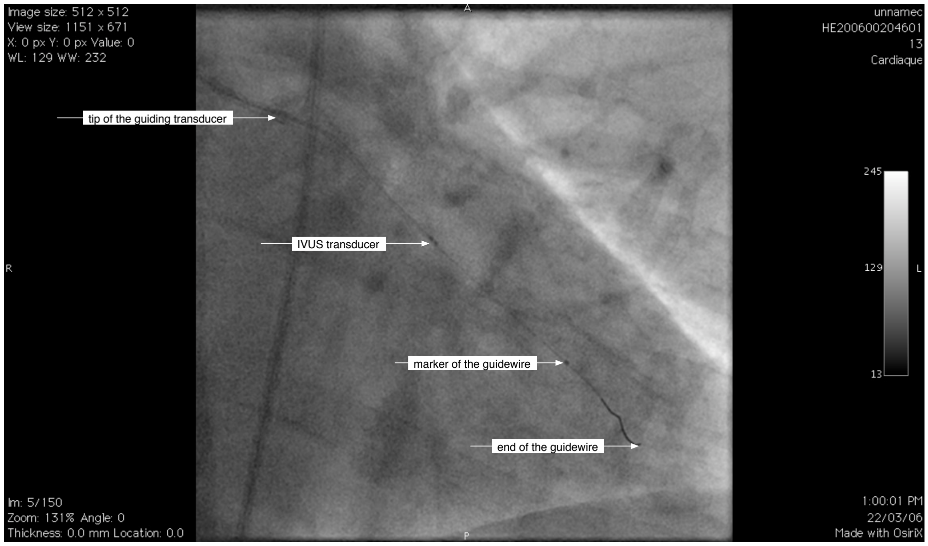

Figure 2: *Features points used as anchor points to the positioning of the whole transducer guide.*

coordinates, since, as in figure 4**(b)**, the characteristic points have a coherence higher than the other pixels of the subimage.

The centroid of the set of pixels for which the criterion 3 is true corresponds to the position of the centroid of the searched structure.

For the first image of the sequence, the user gives the approximate positions of the characteristic points. Those user-supplied points can be as far as 10 pixels from the tracked feature in our implementation given that the dimensions of the searching window around each approximate positions is of $35X35$ pixels. That ensured that the feature points were englobed in those searching areas. For the other frames, the approximate positions are set to be the previous computed coordinates. The figure 9 presents the results obtained by our approach.

With this last method, we compute the positions of the feature points along the IVUS transducer guidewire. These coordinates will be used as anchor points and provide an initial position of the points involved in the snake algorithm described in the next section.

3 Positioning of the Transducer Guide Using Snake Algorithm

In order to position the whole catheter and not only some of its feature points, we elaborated a snake algorithm that determines some other positions along the transducer guide. In this section, we first present an overview of the standard snake algorithm to further describe our version of this technique.

3.1 General Presentation of the Snake algorithm

The snake algorithm is an iterative process that minimizes an energy function associated with a model. Throughout the iterations of the algorithm, the model is deformed to fit some structures in an image. It is composed of a set of points v_i, $i \in [0, n]$ embedded on pixels in the image. Those points may be attached to each other by different means of interpolation.

Some displacements are applied to each of the points v_i to minimize an energy (figure 5). A minimum is obtained when the points are aligned to the searched structure. This kind of approach provides an easy way to incorporate *a priori* information to the evolution of the snake form during the segmentation process ([Mignotte and Meunier 2001]).

The energy function is composed of two terms: the intern energy that depends on the geometry of the snake curve, and the extern energy related to the image itself. The energy is determined as follow:

$$E_{snake} = \int_{snake} (\alpha E_{curvature} + \beta E_{img}) ds \tag{4}$$

where the different variables are defined as follow:

1. $E_{curvature}$ is the energy associated with the curvature of the second derivative of the curve formed by the snake points v_i, $i \in [0, n]$
2. E_{img} is the energy term associated with the analyzed image
3. α, β are parameters adjusted by the user depending on the *a priori* information of the models. For example, α should be higher in the case of smooth contour, in order to restrain the model to have a small curvature.

The extern energy E_{img} is often related to the norm of the intensity gradient in the image. The snake should tend to be close to the pixels with the highest intensity gradient to ensure that they are part of an edge (equation 5).

$$E_{ext}(v_i, I) = -||\nabla I(v_i)|| \tag{5}$$

where $\nabla I(v_i)$ is the intensity gradient in the image for the pixel associated with the control point v_i. By subtracting this quantity to the intern energy, we ensure that the snake tends to follow the pixels with highest gradient.

This kind of approach is seldom applicable to segmentation of medical images since they are often noisy and they have weak intensity gradient even on the edges of the different structures observed.

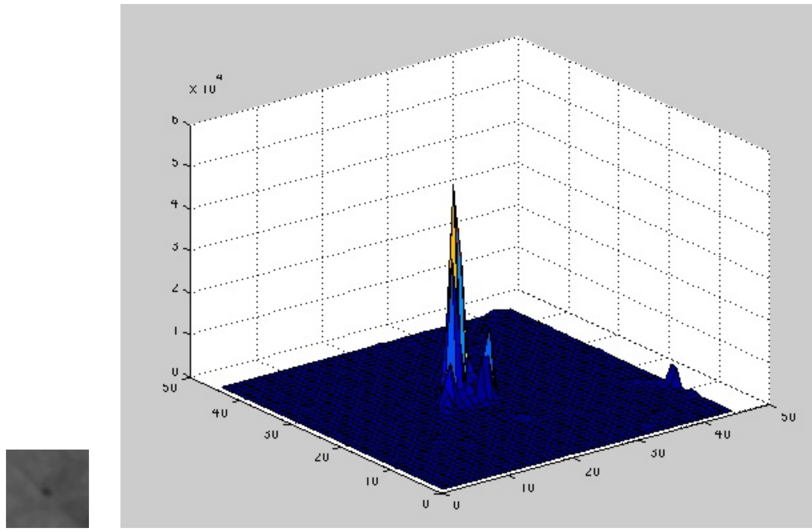

(a) **(b)**

Figure 4: *In* **(a)***, a window of dimensions 35X35 pixels shown with the IVUS transducer. In* **(b)***, the measured coherence associated with the window.*

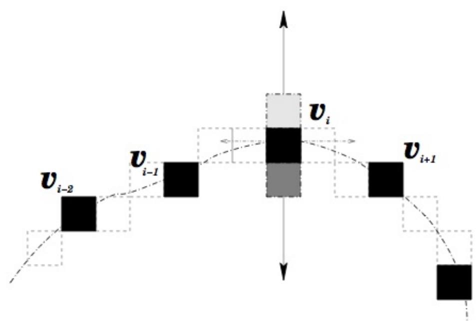

Figure 5: *Displacement of the snake points to obtain a minimal energy.*

3.2 Constrained snake with anchor points

We have elaborated a modified snake method that ensures the automatic positioning of the transducer guidewire throughout fluoroscopic image sequence. The snake used is composed of a set of anchor points for which the minimization process will not influence the position. It is also composed of another set of points that will be positioned according to the minimization of a certain energy function. The fixed points will correspond to the feature points, identified in figure 2, positioned by the tracking method previously described.

The non-fixed points are initially placed equally distanced along a straight line between each pairs of adjacent fixed points. They will be moved to minimize a cost function that depends on the curvature of the snake and the local coherence in the image. Thus, for a snake composed of n unfixed point, we have:

$$E_{snake} = \sum_{i=1}^{n} \Big(\alpha(i) E_{curvature}(i) - \beta(i) E_{img}(i)\Big) \qquad (6)$$

Where:

$$E_{curvature}(i) \quad = \quad |v_{i-1} - 2v_i + v_{i+1}|^2 \qquad (7)$$

$$E_{img}(i) \quad = \quad C(v_i) \qquad (8)$$

We have:

1. $v_i = (x_i, y_i)$ are the different points of the snake.
2. $C(v_i)$ is the coherence found in the image for the coordinates (x_i, y_i) as defined in equation 2.
3. $\alpha(i)$ and $\beta(i)$ are the weights automatically adjusted by a method further described.

We use a greedy strategy to minimize the snake energy. For each v_i unfixed, we compute the energy of each of the pixels contained in a MXM neighborhood surrounding v_i. We move each of the v_i to the position that ensures each of them a minimum energy.

After each v_i has been moved, we compute the value E_{snake}, the energy function for the whole snake as defined in equation 6. The minimization process continues until E_{snake} stops decreasing, indicating that a minimum has been reached.

The algorithm is applied to each of the image of the sequence. For the first frame, the approximate positions of the different feature points along the transducer guide are provided by the user, as mentioned in the previous section. For the remaining frames of the sequence, these approximate coordinates are the positions of the feature points in the previous frame.

3.2.1 Automatic Adjustment of the Parameters of the Snake

In the energy function, the parameters $\alpha(i)$ and $\beta(i)$ have to be set. Some parts of the transducer guidewire may seem to disappear due to a low contrast with the background (figure 6). There are also points for which we compute a high coherence when they are part of noisy stain of the background (figure 7).

For a point v_i in such a region, we would accord a higher importance to $E_{curvature}(i)$ by setting $\alpha(i)$ smaller than $\beta(i)$ in the equation 6. To do so, we have to detect situations for which the information $E_{img}(i)$ is not reliable.

We base our approach on the eigenvectors v_1, v_2 of the matrices J_0 defined in the equation 1. Considering that the curvature of the

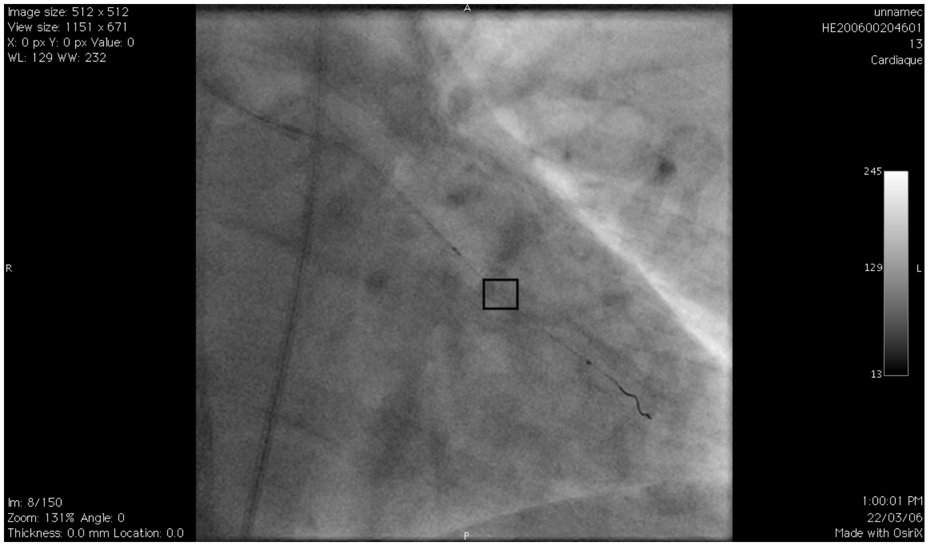

Figure 6: *The part of the IVUS transducer guidewire is almost imperceptible because of its low contrast with the background*

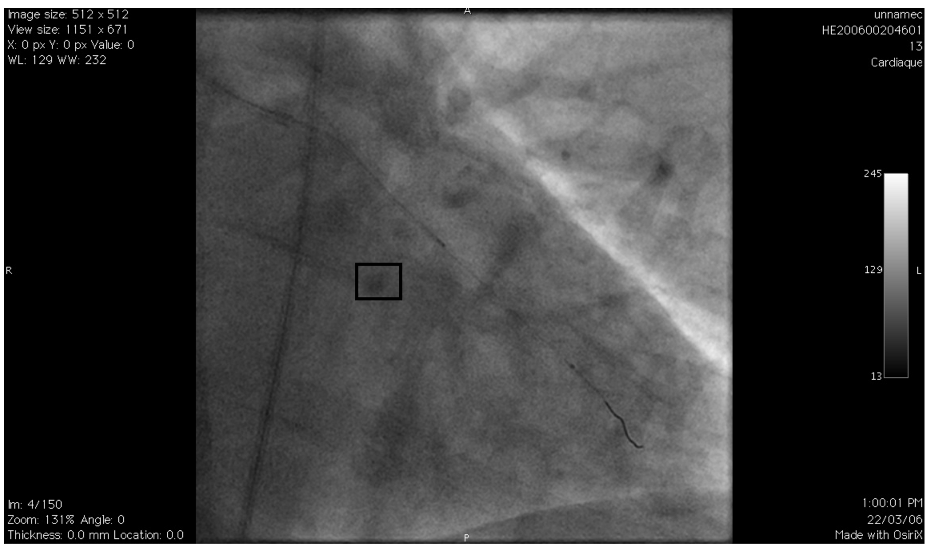

(a)

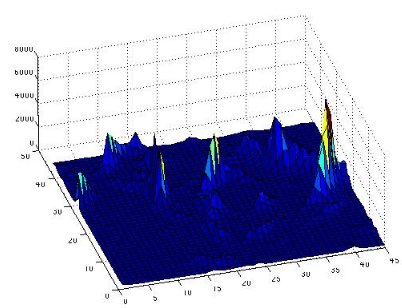

(b)

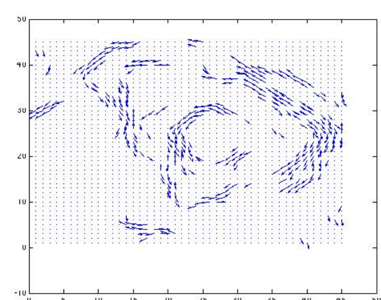

(c)

Figure 7: *In* **(a)***, a noisy stain is indicated by a black square. In* **(b)***, the coherence surface computed for the region marked in* **(a)***. In* **(c)***, the vectors v_2 associated with high coherence points of* **(b)***.*

guidewire is small in restrained portions of it, the pixels directly on its edges should have their gradient directions closed to each other.

We see, in the figure 8 **(b)** and **(c)**, the coherence surface and the eigenvectors v_2 of high coherence points associated with a small window containing a part of the guidewire.

Thus, we determine a pixel (x, y) to be part of the guidewire if :

1. $C(x, y)$ is higher than the mean coherence $\overline{C}$ in a neighborhood of this pixel
2. (x, y) is surrounded by neighbors with high coherence
3. (x, y) is surrounded by neighbors for which the direction of the associated vector v_2 are in a vicinity of the one related to (x, y).

We define a set S of points that are part of a neighborhood of v_i and have a coherence C higher than the mean coherence $\overline{C}$ found in that neighborhood.

Thus, we determine a set of points S for which coherence is higher than the mean coherence in the neighborhood of the point v_i. For each of the points $s_i \in S$, we attribute a value $A(i)$ defined as follow:

$$A(i) = \sum_{s \in N} a(s) \tag{9}$$

$$a(s) = \begin{cases} 1 & \text{if } |\theta_s - \theta_i| < T \\ 0 & \text{otherwise} \end{cases} \tag{10}$$

Where θ_s is the direction of the vector v_2 for the point $s \in S$.

We can see the results of this accumulation in the figure 8(**d**). The brightest points are associated with high value of $A(i)$ meaning that they have other points in their neighborhood which are part of S and have slightly the same eigenvectors direction v_1 and v_2.

This last accumulation function allows us to determine if a region of the image is only composed of noisy stain as shown in figure 7, or if it actually contains a part of the guidewire, which would lead to a higher value of $\beta(i)$. From the values of $A(i)$, we can determine a new set $S' \subset S$ of points that are relevant. To do so, we just keep the points $i \in S$ which satisfy the condition:

$$A(s) \geq T$$

Where T is a threshold determined empirically and was set to 10 ensuring that points in S' are all part of an oriented structure in the image. We determined this last value by setting T proportional to the area covered by the neighborhood implied in the processing of the $A(s)$.

As shown in figure 8(**d**), the points which have a high value for $A(i)$ should be highly spatially correlated since they are almost aligned along a line. To determine if the points $s \in S'$ are just associated with noise in the image or the guidewire, we compute their covariance which measures the strength of their correlation:

$$cov(x, y) = \sum_{i=1}^{N} \frac{(x_i - \overline{x})(y_i - \overline{y})}{N} \tag{11}$$

where

- x_i,y_i are the coordinates of the points in S'
- $\overline{x}$, $\overline{y}$ are respectively the mean for X-coordinates and Y-coordinates for points in S'
- N is the number of points in S'

The absolute value of equation 11 reaches a maximum of 1 when the points in S' are perfectly aligned along a line indicating that they are highly likely to be part of the transducer guidewire. When the points in S' are sparse and not correlated, the absolute value of their spatial covariance will tend to be 0. Hence, we set:

$$\alpha(i) = |cov(x_{S'(i)}, y_{S'(i)})| \tag{12}$$

$$\beta(i) = 1 - \alpha(i) \tag{13}$$

where $x_{S'(i)}$,$y_{S'(i)}$ are the coordinates of the points contained in the computed set S' in a neighborhood of v_i.

Finally, we set $\alpha = 1 - \beta$, which will automatically lead to a high value of α when β is low, indicating that the information from the image is not reliable.

4 Results and discussion

The method presented in this paper has been tested on a fluoroscopic image sequence of 150 frames, provided by the Montreal Heart Institute. In this section we present the results for the tracking and snake algorithm.

4.1 Feature point tracking

In the figure 9, we show the results obtained for the feature point tracking. We can see that the algorithm finds a right position for each of the characteristic points, even if the points clicked are not directly on the structures we want to track. As long as the searching window around the given approximate position is big enough to contain the structures, the algorithm retrieves the centroid of the tracked elements of the image.

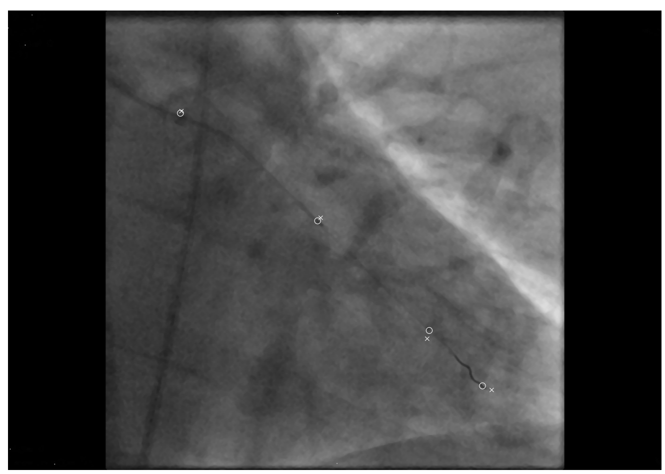

Figure 9: *Results of the feature point tracking method. The "X" are the clicked points by the user, and the "O" are the feature points coordinates computed.*

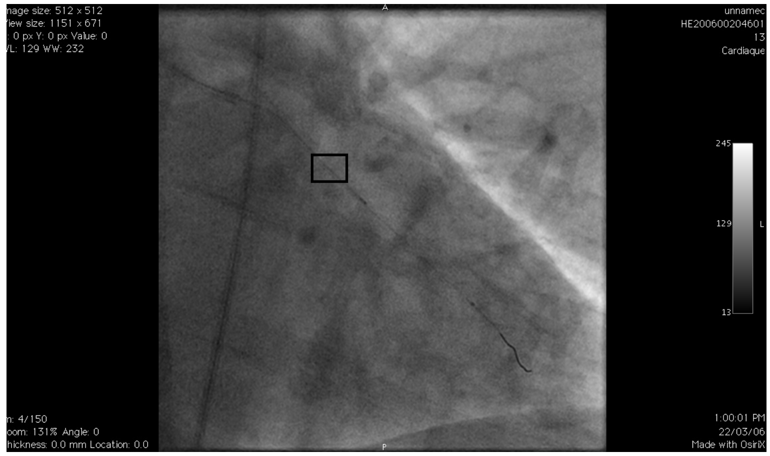

(a)

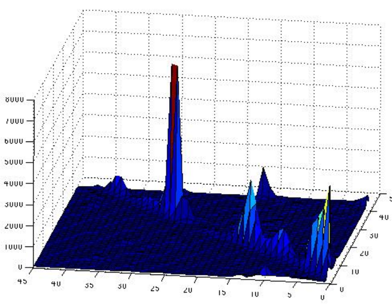

(b)

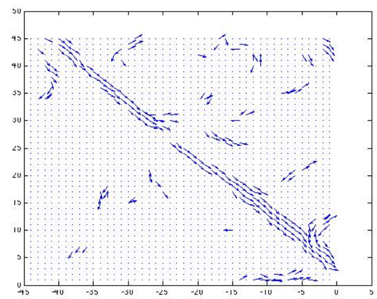

(c)

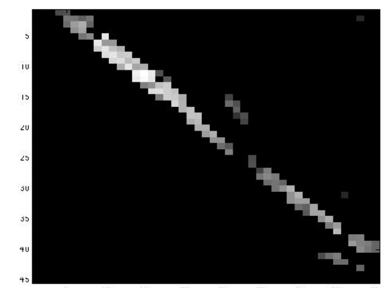

(d)

Figure 8: *In* **(a)***, a part of the guidewire of the transducer. In* **(b)***, the coherence surface computed for the region marked in* **(a)***. In* **(c)** *and* **(d)** *respectively, the vectors* v_2 *and the function* $A(i)$*, associated with high coherence points in the region marked in* **(a)***.*

4.2 Snake Algorithm result

We show, in the figure 10, some frames with snake results illustrated in red. To obtain a full curve along the snake, we interpolated points by a cubic Hermite interpolation. We can see that the snake fits the transducer guidewire even when this one is at its maximum curvature for the whole sequence of images.

The part of the transducer which was most likely to have a small contrast with the background was found between the IVUS transducer and the marker on the guidewire (figure 10 **(a)** and **(b)**). We can notice that it is well-fitted by the snake curve, demonstrating the efficiency of our algorithm to recover the low-contrast shapes.

5 Conclusion

This research has investigated the problem of localization of an IVUS transducer guidewire using a snake-based method. The snake is constrained by anchor points aligned on some features in the images. We also provide a method to automatically adjust the weighting parameters of the different parts of the snake-energy function to minimize. The method works even when there is a low contrast between some parts of the tracked structure and the background of the images. Our method is a first step to the elaboration of a full registration technique of an IVUS guidewire throughout a single-plane fluoroscopic sequence of images.

Acknowledgments

This work was supported by the National Sciences and Engineering Research Council of Canada(NSERC) and the Montreal Heart Institute(MHI).

References

JOURDAIN, M., MEUNIER, J., MONGRAIN, R., SHERKNIE, D., WENG, J. Y., AND TARDIF, J.-C. 2004. 3d reconstruction of an ivus transducer trajectory with a single view in cineangiography. In *SPIE Medical Imaging 2004*, SPIE.

J.ROELANDT, MARIO, C., G.N.PANDIAN, WENGUANG, L., D.KEANE, SLAGER, J., DE FEYTER, J., AND P.W.SERRUYS. 1994. Three-dimensional reconstruction of intracoronary ultrasound images: Rationale,approaches, problems, and direction. *Circulation 90*, 1, 1044–1055.

LABAN, M., OMEN, J., AND SLAGER, J. 1995. Angus: a new approach to three dimensional reconstruction of coronary vessels by combined use of angiography and intravascular ultrasound. *Computers in cardiology Piscataway, NJ:IEEE Computer Society*, 325–328.

MIGNOTTE, M., AND MEUNIER, J. 2001. A multiscale optimization approach for the dynamic contour-based boudary detection issue. *Computerized Medical Imaging and Graphics 25*, 3 (May), 265–275.

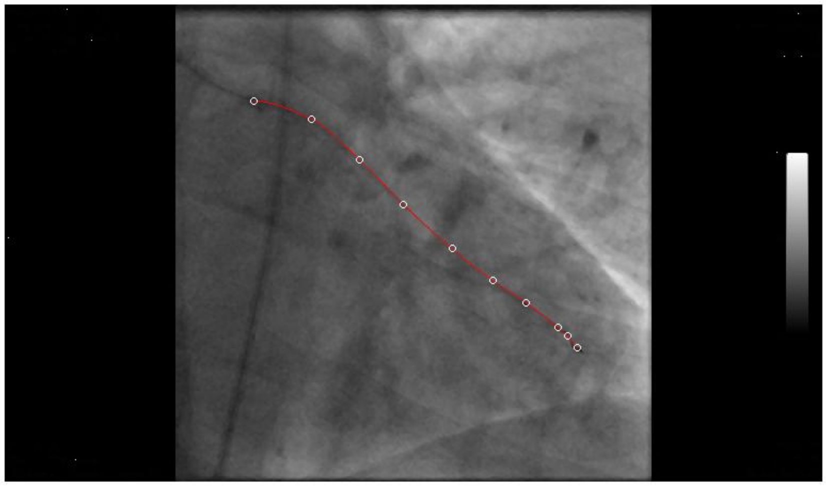

(a)

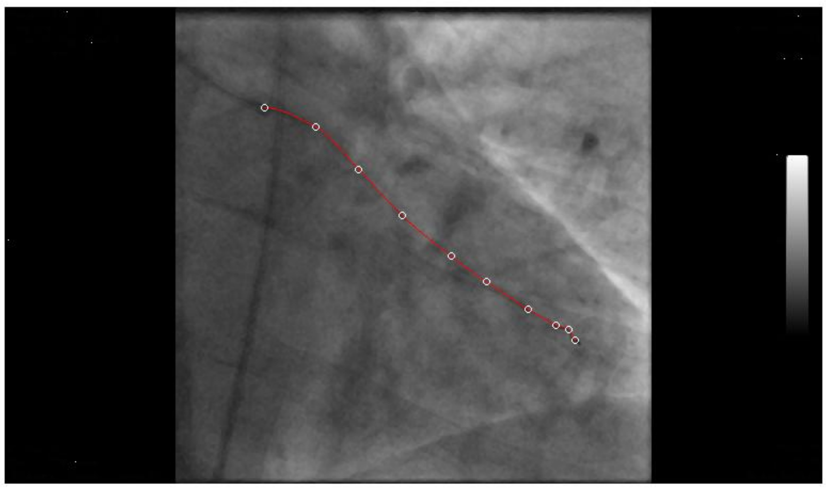

(b)

Figure 10: *Results obtained for the snake algorithm on some images of the fluoroscopic images*

SHERKNIE, D., MEUNIER, J., MONGRAIN, R., AND TARDIF, J.-C. 2005. Three-dimensional trajectory assessment of an ivus transducer from single-plane cineangiograms: A phantom study. *IEEE Transactions on Biomedical Engineering 52*, 3, 543–549.

SLAGER, J., WENTZEL, J. J., SCHUURBIERS, J. C. H., OMEN, J., KLOET, J., KRAMS, R., VON BIRGELEN, C., VAN DER GIESSEN, W. J., SERRUYS, P., AND DE FEYTER, P. J. 2000. True 3-dimensional reconstruction of coronary arteries in patients by fusion of angiography and ivus(angus) and its quantitative validatio. *Circulation 102*, 511–516.

WAHLE, A., G.P.M.PRAUSE, DEJONG, S. C., AND SONKA, M. 1999. Geometrically correct 3-d reconstruction of intravascular ultrasound images by fusion with biplane angiography-methods and validation. *IEEE Transactions on Medical Imaging 18*, 8, 686–699.

WEICKERT, J. 1998. *Anisotropic Diffusion in Image Processing*. B.G. Teubner Stuttgart.